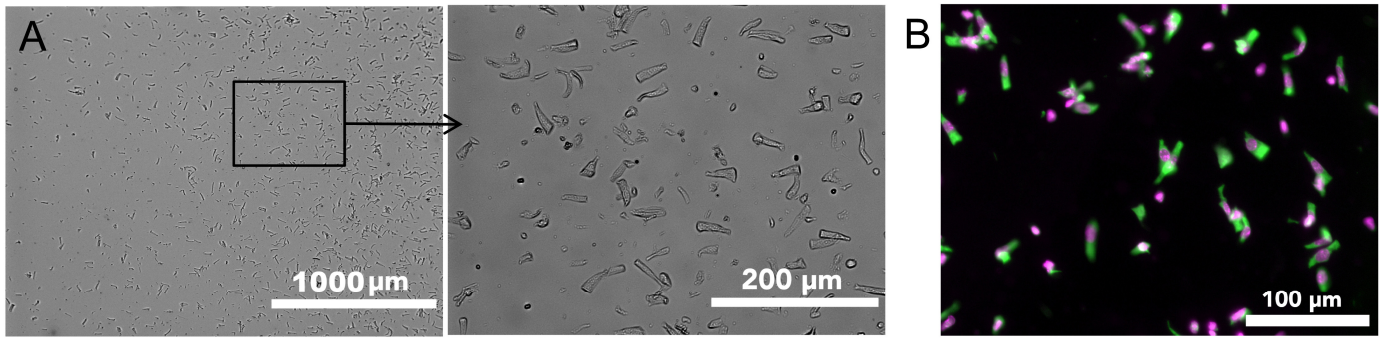

Fig. S1. Imaging of single cell suspensions prepared by FFPE-DISSECT from embedded mouse intestinal tissue by brightfield and autofluorescence. (A) Brightfield imaging of whole columnar epithelial cells isolated as single cells. **(B)** Fluorescence imaging of column epithelial cells as single cells using Hoescht (nuclei - magenta) and autofluorescence (green). Images are representative of 3 experiments. Scale bars as indicated.

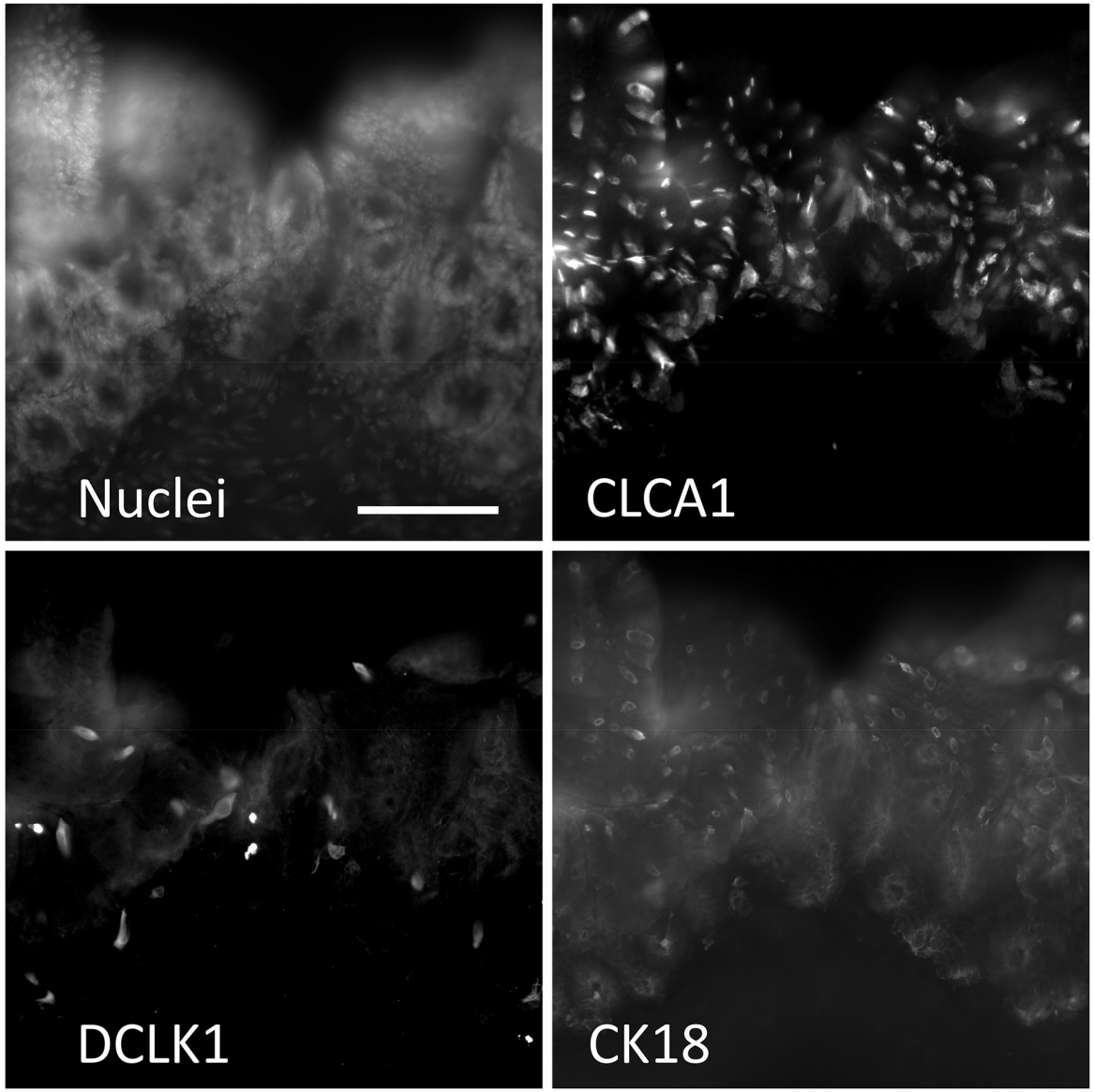

Fig. S2. Whole mount staining of embedded mouse intestinal tissue prepared by FFPE-DISSECT before single cell disaggregation. Whole mount immunofluorescence staining for cell type markers (CK18, CLCA1, DCLK1). Images are representative of 3 experiments. Scale bars, 100 μm.

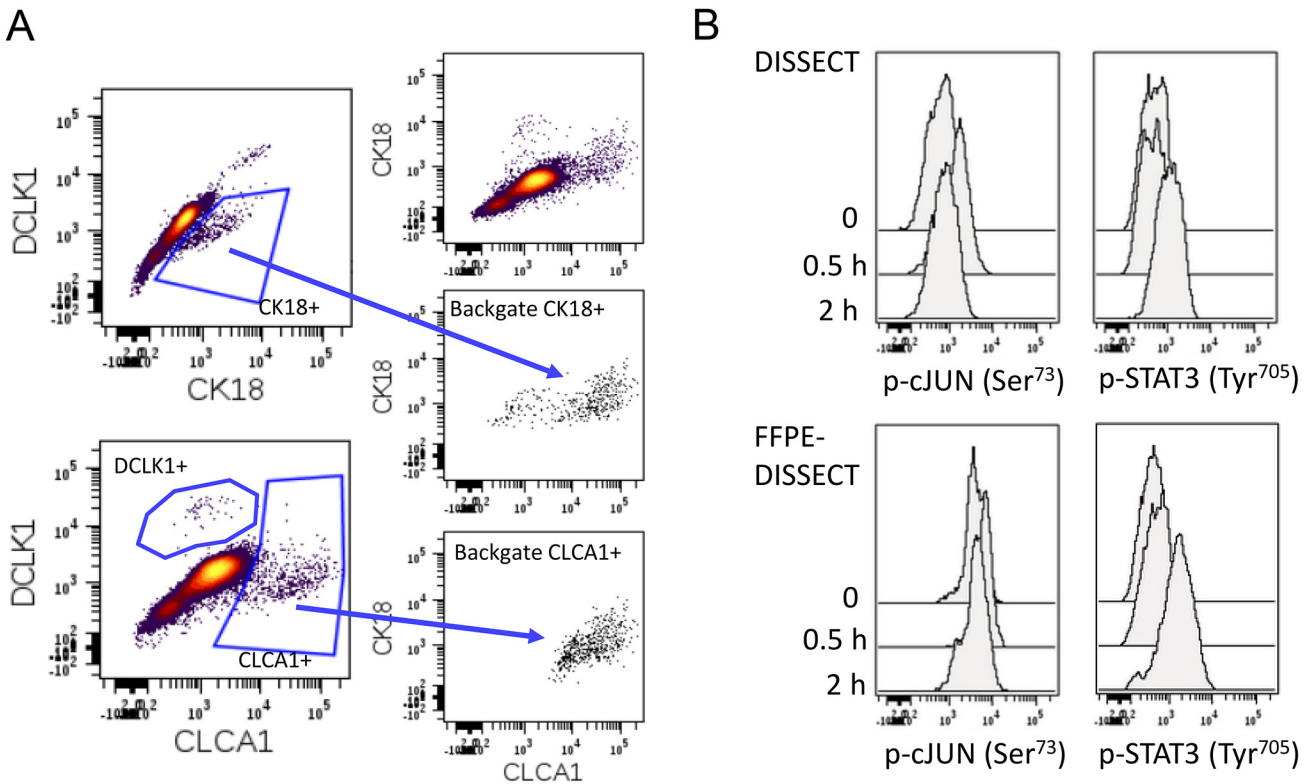

Fig. S3. Fluorescence cytometry of samples prepared by FFPE-DISSECT. (A) Flow cytometry bi-plots of the mouse duodenum prepared by FFPE-DISSECT. Manual gating of goblet cells by CK18 and CLCA1, and tuft cells by DCLK1. CK18 and CLCA1 singular positive cells are back-gated to a bi-axial plot not used for the original gating to demonstrate that the cells comprise an overlapping goblet cell population. **(B)** Phospho-flow analysis of p-cJUN (early signal) and p-STAT3 (late signal) of the murine duodenum in response to TNF-α at specified time points. Single cells were prepared either immediately by DISSECT, or FFPE-embedded and then by FFPE-DISSECT. Data are representative of 3 experiments.

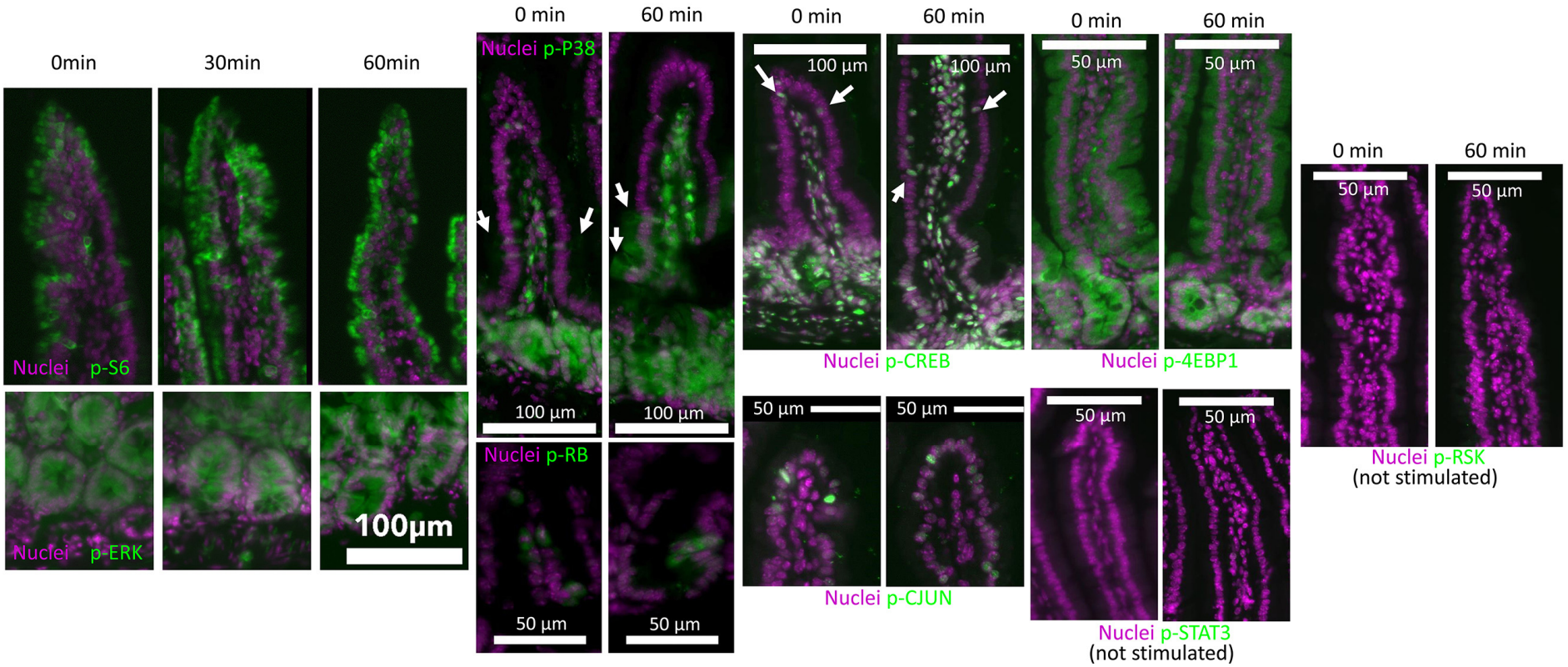

Fig. S4. Signals are preserved for up to 1 hour post-excision. Immunofluorescence imaging of basal signals for all phospho-protein signaling markers used in the human study (Table S3) in FFPE murine tissues with a post-excision time of up to one hour for simulating possible tissue preparation conditions in the human study. Murine duodenal tissues were harvested, and then either fixed immediately, or stored in RPMI for 30 or 60 minutes (as per Cooperative Human Tissue Network standard operating procedure) prior to fixation and FFPE processing. Crypts, villi, or both displayed according to signal localization. Arrows represent individual positive cells. Images are representative of 3 experiments. Scale bars as indicated.

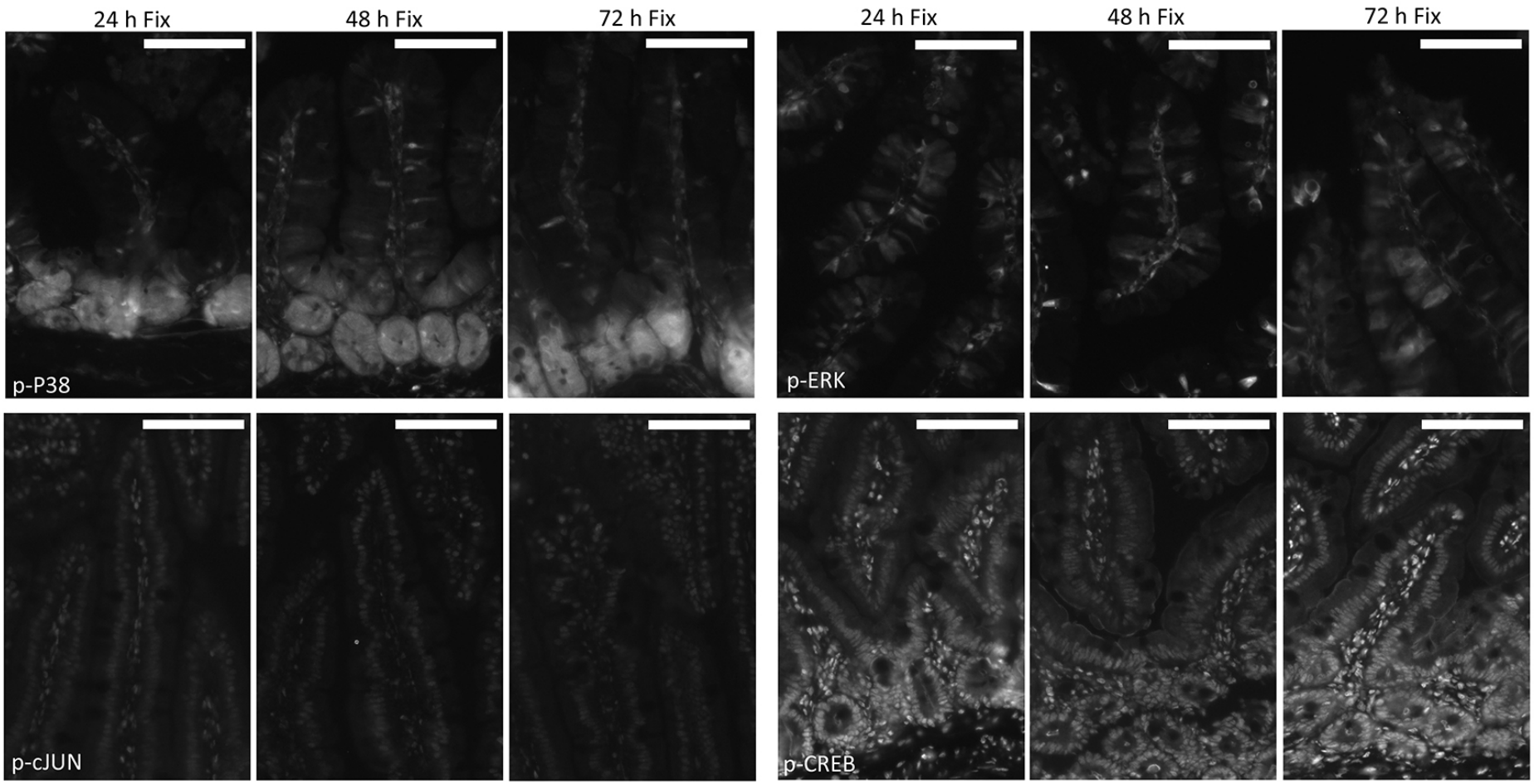

Fig. S5. Fixation time does not affect signaling marker detection in FFPE. Immunofluorescence imaging of murine duodenal tissues stimulated by TNFα for 30 mins that were in fixative for the indicated time. Representative cytoplasmic (p-P38, p-ERK) and nuclear (p-cJUN, p-CREB) signals from 3 experiments. Scale bars, 100 μm.

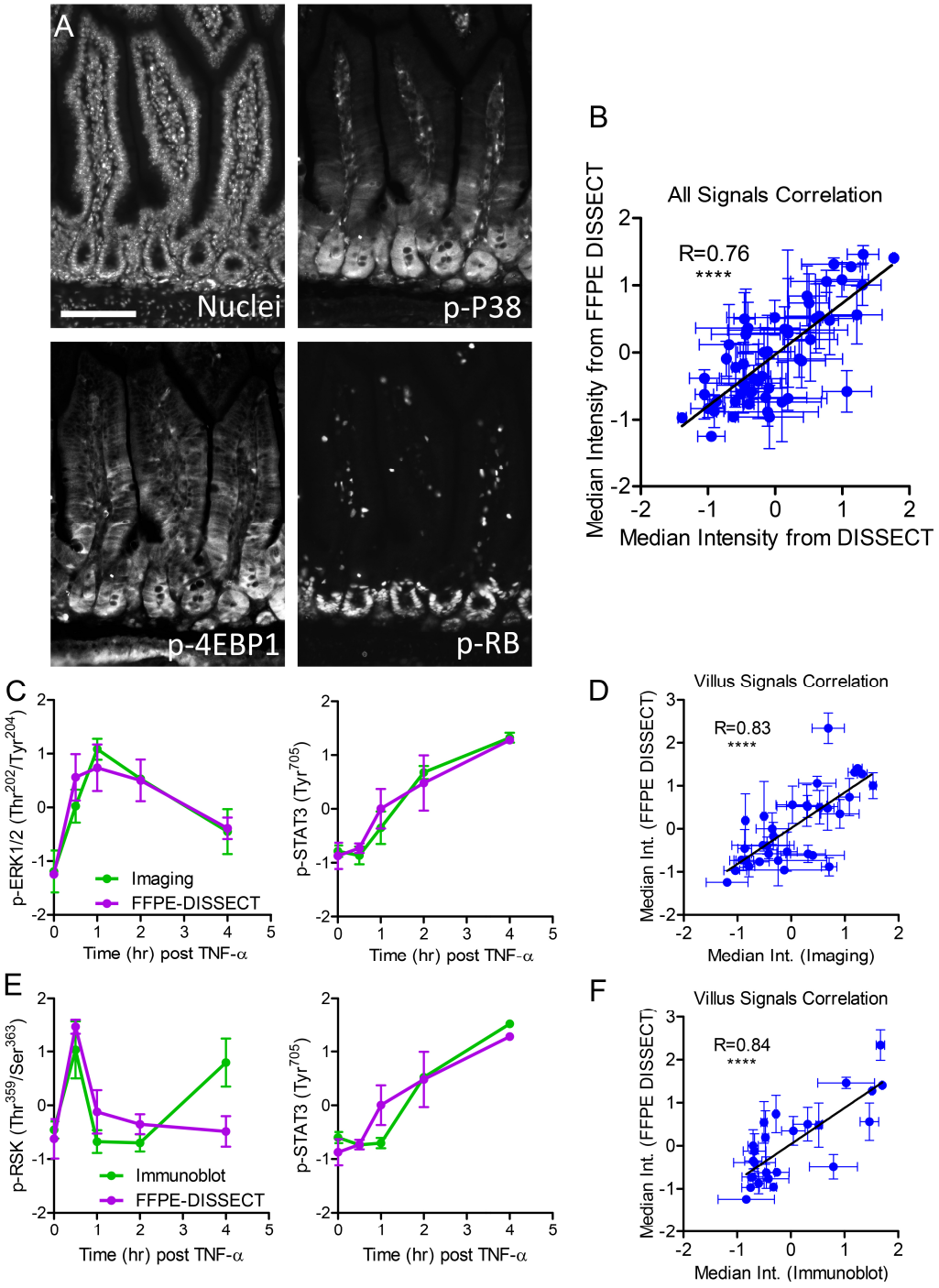
A
Nuclei
p-P38
p-4EBP1
p-RB
B
All Signals Correlation
R=0.76
****
Median Intensity from FFPE DISSECT
Median Intensity from DISSECT
C
p-ERK1/2 (Thr202/Tyr204)
Imaging
FFPE-DISSECT
Time (hr) post TNF-α
p-STAT3 (Tyr705)
Time (hr) post TNF-α
D
Villus Signals Correlation
R=0.83
****
Median Int. (FFPE DISSECT)
Median Int. (Imaging)
E
p-RSK (Thr359/Ser363)
Immunoblot
FFPE-DISSECT
Time (hr) post TNF-α
p-STAT3 (Tyr705)
Time (hr) post TNF-α
F
Villus Signals Correlation
R=0.84
****
Median Int. (FFPE DISSECT)
Median Int. (Immunoblot)

Fig. S6. Villus signal comparison between FFPE-DISSECT, quantitative imaging, quantitative immunoblotting. (A) Immunofluorescence imaging of p-P38, p-4EBP1, p-RB at baseline without stimulation in murine duodenal FFPE sections. Scale bars, 100 μm. **(B)** Correlation analysis combining all signaling markers (both villus and crypt), comparing mass cytometry data generated by DISSECT against FFPE-DISSECT. **(C)** Quantitative comparisons of measurements obtained by immunofluorescent imaging of FFPE tissue sections versus FFPE-DISSECT-mass cytometry on two different cohorts of mice. Duodenal tissues were used. Representative of early (p-ERK) and late (p-STAT3) signals. **(D)** Correlation analysis of combined villus signaling markers (CC3, p-STAT3, p-cJUN, p-ATF2, p-CREB, p-ERK, p-S6), comparing immunofluorescent imaging data against mass cytometry data generated by FFPE-DISSECT. **(E)** Quantitative comparisons of measurements obtained by immunoblotting using fresh tissue versus FFPE-DISSECT-mass cytometry on two different cohorts of mice. Duodenal tissues were used. Representative of early (p-RSK) and late (p-STAT3) signals. **(F)** Correlation analysis of combined villus signaling markers (p-RSK, CC3, p-STAT3, p-ERK, p-S6), comparing immunoblotting data against mass cytometry data generated by FFPE-DISSECT. Error bars represent SEM from n=3 animals. Data scales are Z-score values derived from mean centering and variance scaling of each set of time course experiment. **** $P \leq 0.0001$ from t-test.

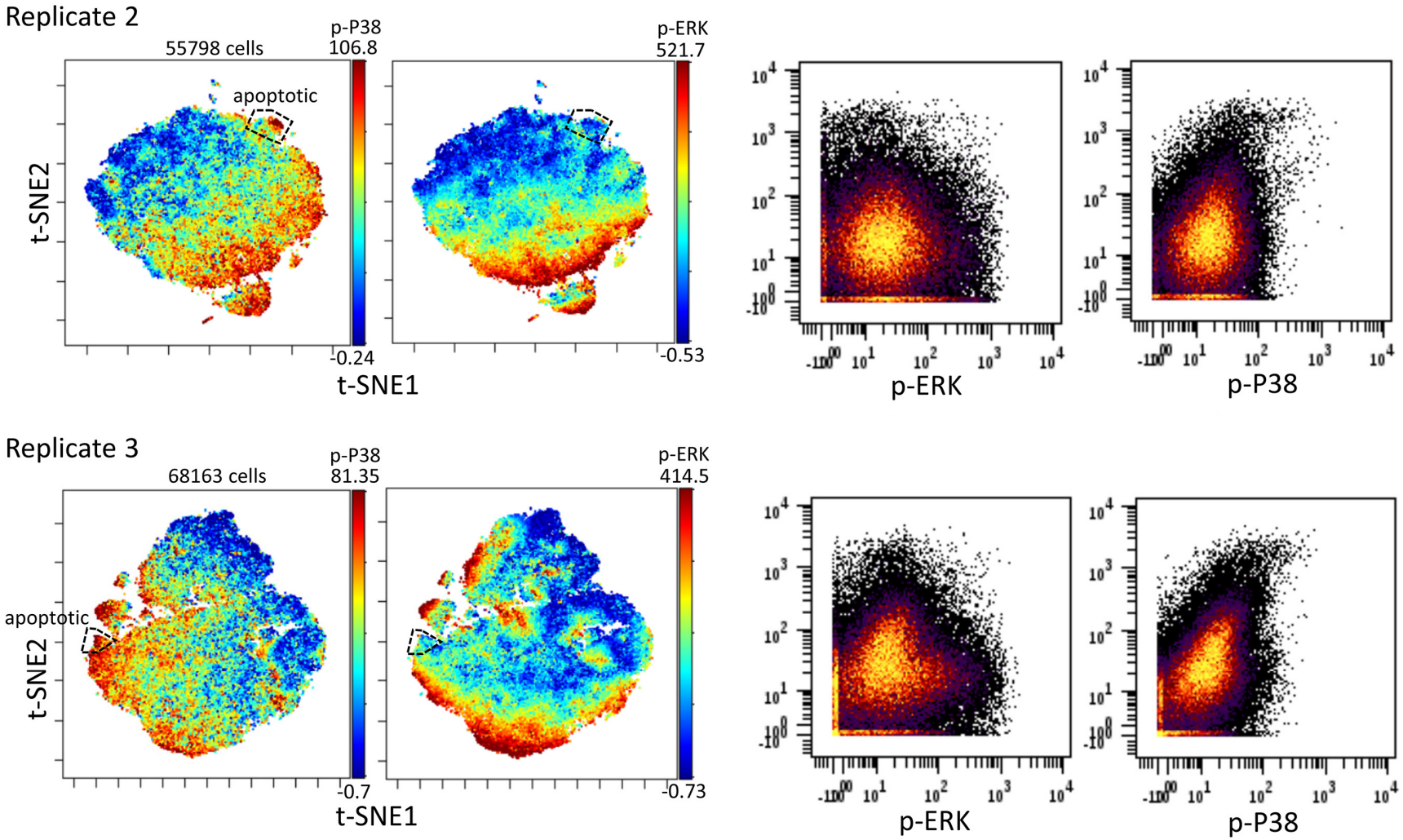

Fig. S7. Replicates over multiple animals depicting relationships between apoptosis and signaling pathways using t-SNE and bi-plots. t-SNE analysis of mass cytometry data from the mouse duodenum exposed to TNF-α for 1 hr, prepared by FFPE-DISSECT. Color overlaid represents the relative quantification of cleaved caspase 3, p-ERK, and p-P38 events, respectively. Labelled cells: apoptotic – CC3+ (A) 2.07%, (B) 2.09%. Numbers on right axis represent min and max value of the color scale. Data representative of n=3 animals (see Fig. 4A, B).

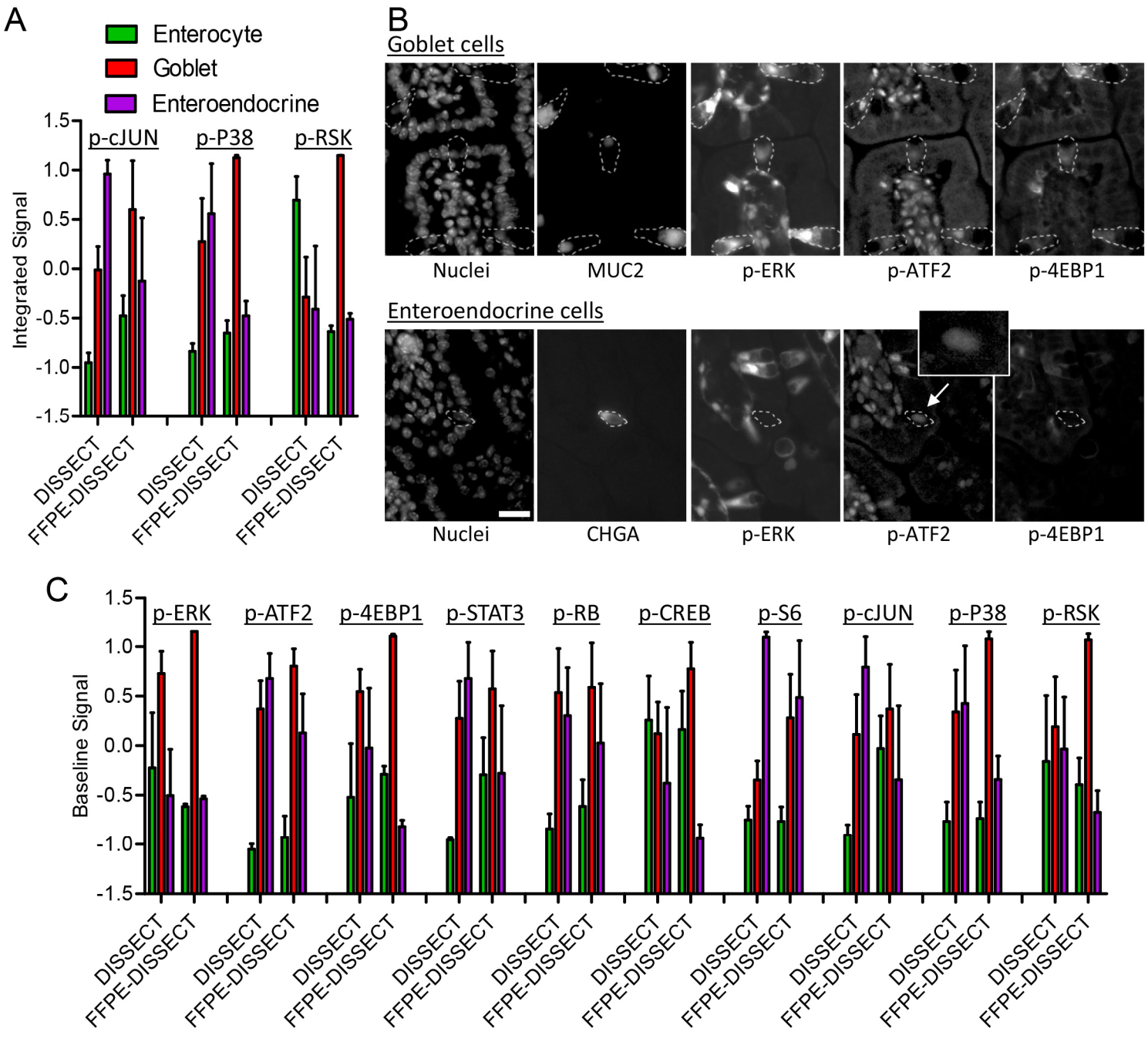
A
Enterocyte
Goblet
Enteroendocrine
p-cJUN
p-P38
p-RSK
Integrated Signal
1.5
1.0
0.5
0.0
-0.5
-1.0
-1.5
DISSECT
FFPE-DISSECT
B
Goblet cells
Nuclei
MUC2
p-ERK
p-ATF2
p-4EBP1
Enteroendocrine cells
Nuclei
CHGA
p-ERK
p-ATF2
p-4EBP1
C
p-ERK
p-ATF2
p-4EBP1
p-STAT3
p-RB
p-CREB
p-S6
p-cJUN
p-P38
p-RSK
Baseline Signal
1.5
1.0
0.5
0.0
-0.5
-1.0
-1.5
DISSECT
FFPE-DISSECT

Fig. S8. Cell type-specific signaling in the murine duodenal epithelium. (A) A subset of signals specific to epithelial cell types (enterocyte- CK20+, CLCA1-, CHGA-, goblet – CLCA1+, enteroendocrine – CHGA+) calculated by integrating signal values over the entire TNF-α time course, comparing mass cytometry data generated by DISSECT against FFPE-DISSECT. **(B)** Replicate IF imaging to confirm cell type-specific signals (p-ERK, p-ATF2, p-4EBP1) at baseline. Scale bars, 20 μm. **(C)** Baseline signals specific to epithelial cell types, comparing mass cytometry data generated by DISSECT against FFPE-DISSECT. Error bars represent SEM from n=3 animals, and data scales are Z-score values derived from mean centering and variance scaling over data values for the three cell types for each method.

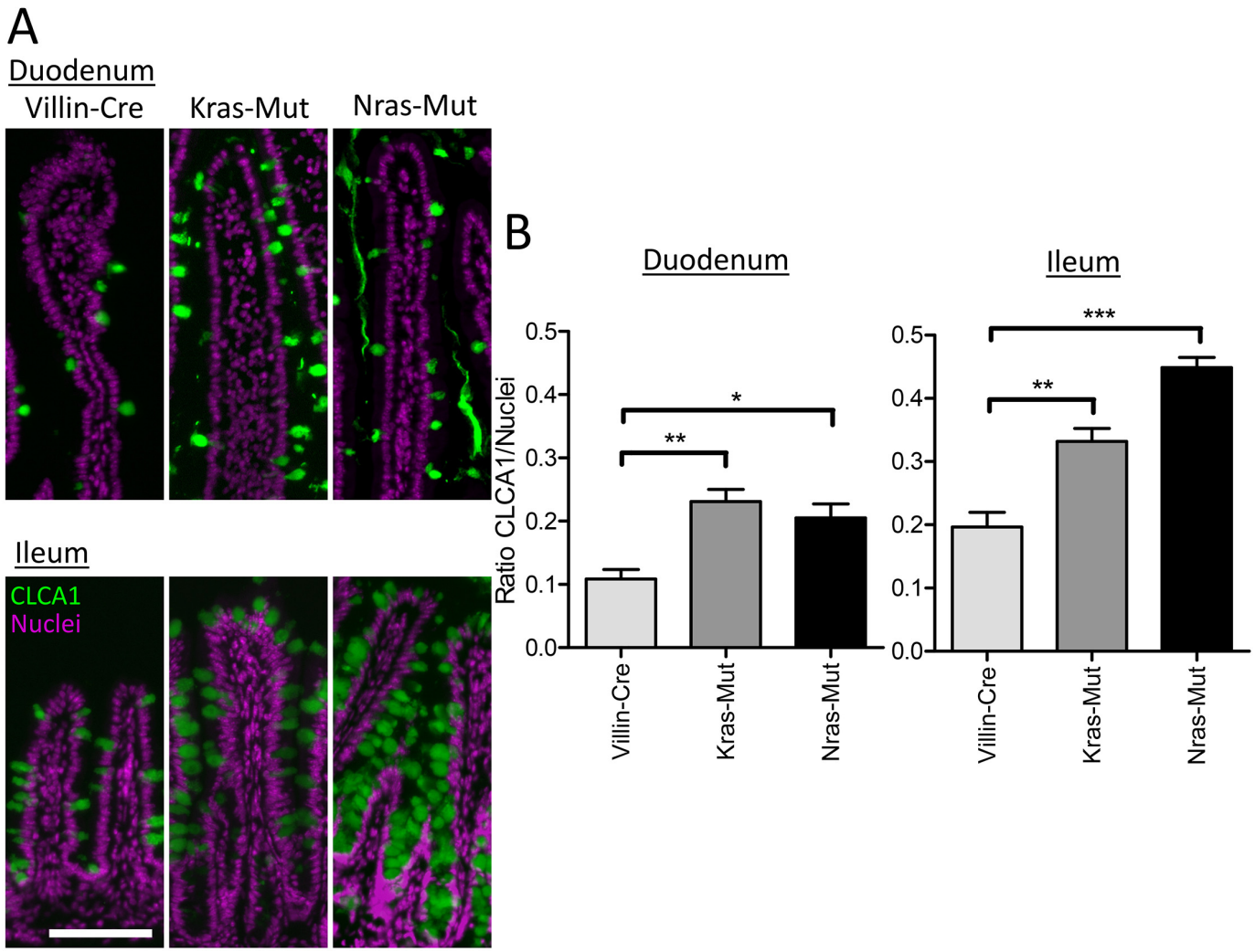

Fig. S9. RAS induction of MEK-ERK signaling induces goblet cell identity. (A) Immunofluorescence imaging of goblet cells by CLCA1 staining in *Villin-Cre*/+ control (Villin-Cre), *Villin-Cre*/+; $KRas^{LSL\text{-}G12D/+}$ (Kras-Mut), and *Villin-Cre*/+; $NRas^{LSL\text{-}G12D/+}$ (Nras-Mut) murine duodenal and ileal epithelial. (B) Quantification of the ratio of area occupied by CLCA1 staining versus nuclear staining in the villus (with a correction factor for the size of a goblet granule against the size of a nucleus). Scale bars, 100 μm. Error bars represent SEM from n=3 animals.

MSS *KRAS* WT (33473)

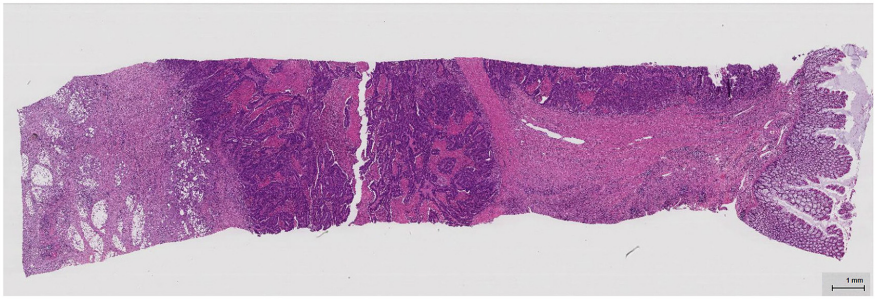

MSS *KRAS* Mut (33482)

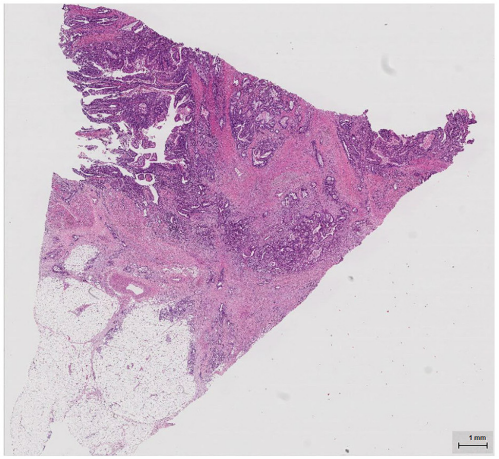

MSI *BRAF* WT (33476)

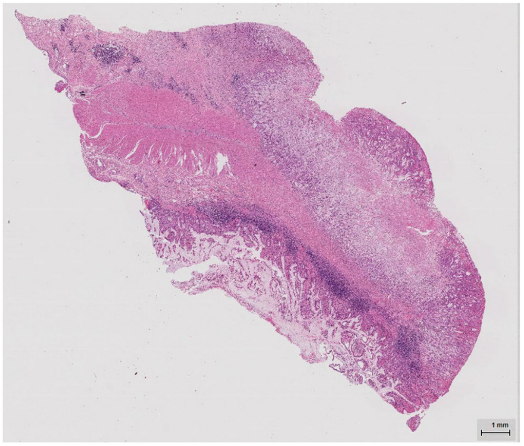

MSI *BRAF* Mut (33471)

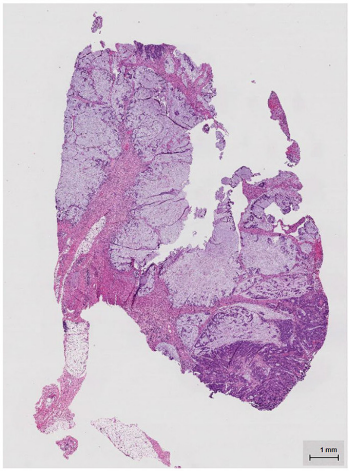

Fig. S10. Hematoxylin and eosin of MSS and MSI CRCs showing tissue areas occupied by tumors. Low magnification view of tumor sections from FFPE blocks for representative MSS and MSI CRC with or without mutant *KRAS* or *BRAF*, respectively. Scale bars, 1 mm. Data representative of n>6 human patient samples for each group (MSS-CRC, MSI-CRC).

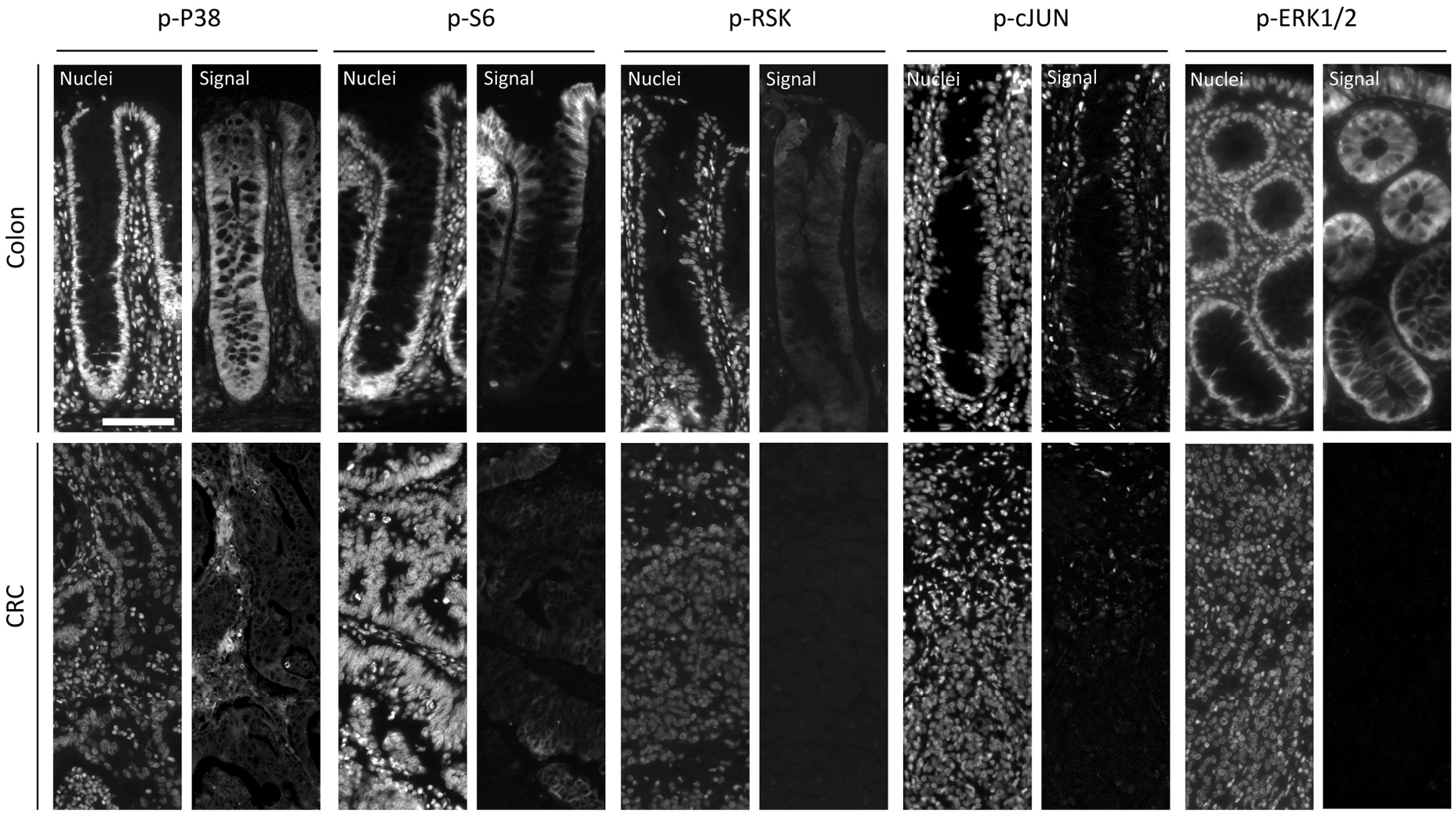

Fig. S11. Signaling in human normal colon and CRC. Immunofluorescence imaging of p-P38, p-S6, p-P90RSK, p-cJUN, and p-ERK1/2 in human colon and CRC FFPE samples, with full representation of the surface-to-crypt axis. Left = nuclei, right = signals. Scale bars, 100 μm. Data representative of n>6 human patient samples for each group (colon, MSS-CRC, MSI-CRC).

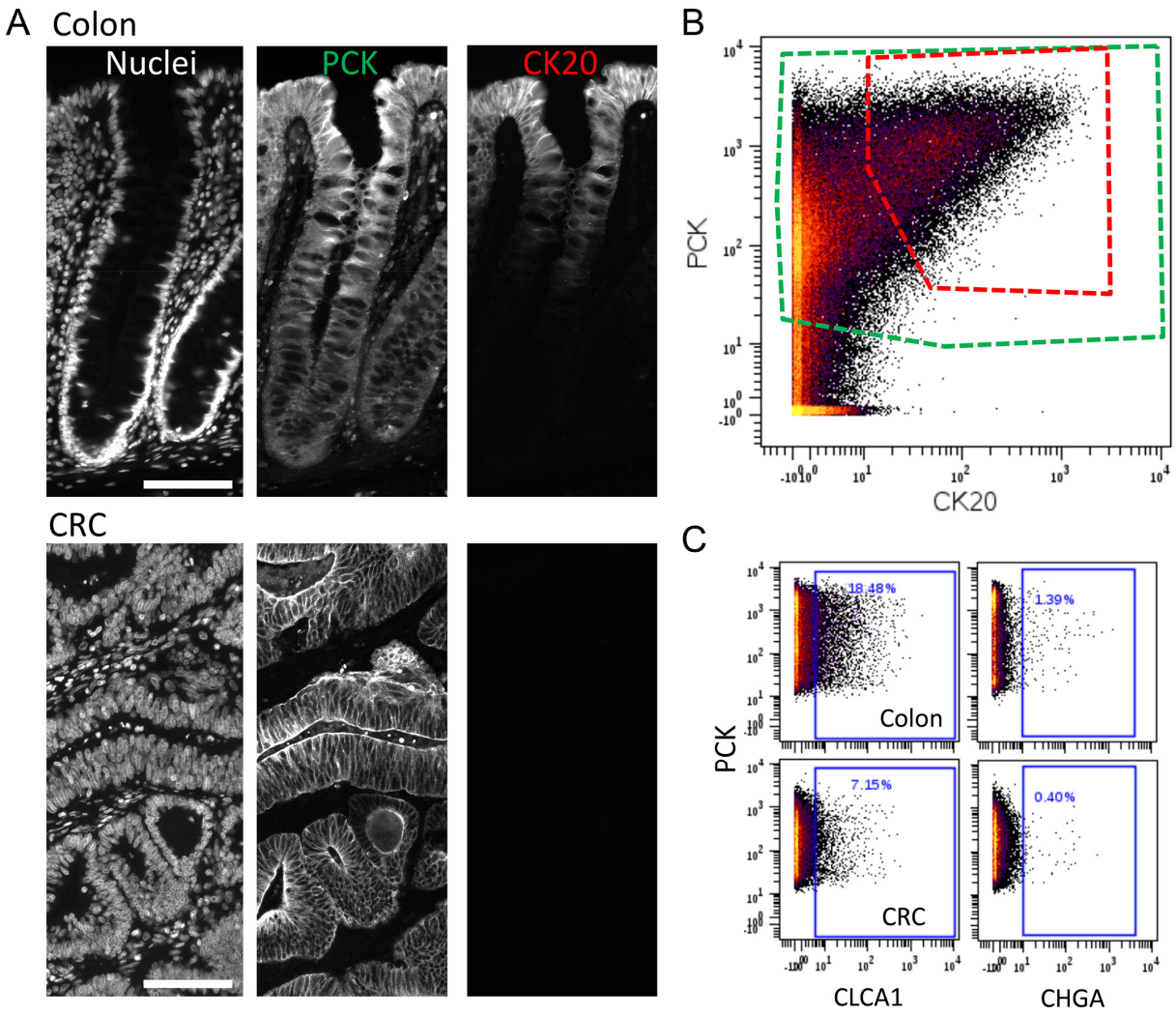

Fig. S12. Differentiation in human normal colon and CRC. (A) IF imaging of PCK, which marks all epithelial cells, and CK20, which marks differentiated epithelial cells in normal colon and CRC. Scale bars, 100 μm. **(B)** Mass cytometry-generated bi-plot of PCK vs. CK20 abundances in normal colonic cells overlaid with cell density. Schematic of epithelial (tumor) cell gating by PCK (green) and CK20 (red) for further analysis. **(C)** Manual gating of goblet cells by CLCA1 and enteroendocrine cells by CHGA for normal colon and CRC. Data representative of n>6 human patient samples for each group (colon, MSS-CRC, MSI-CRC).

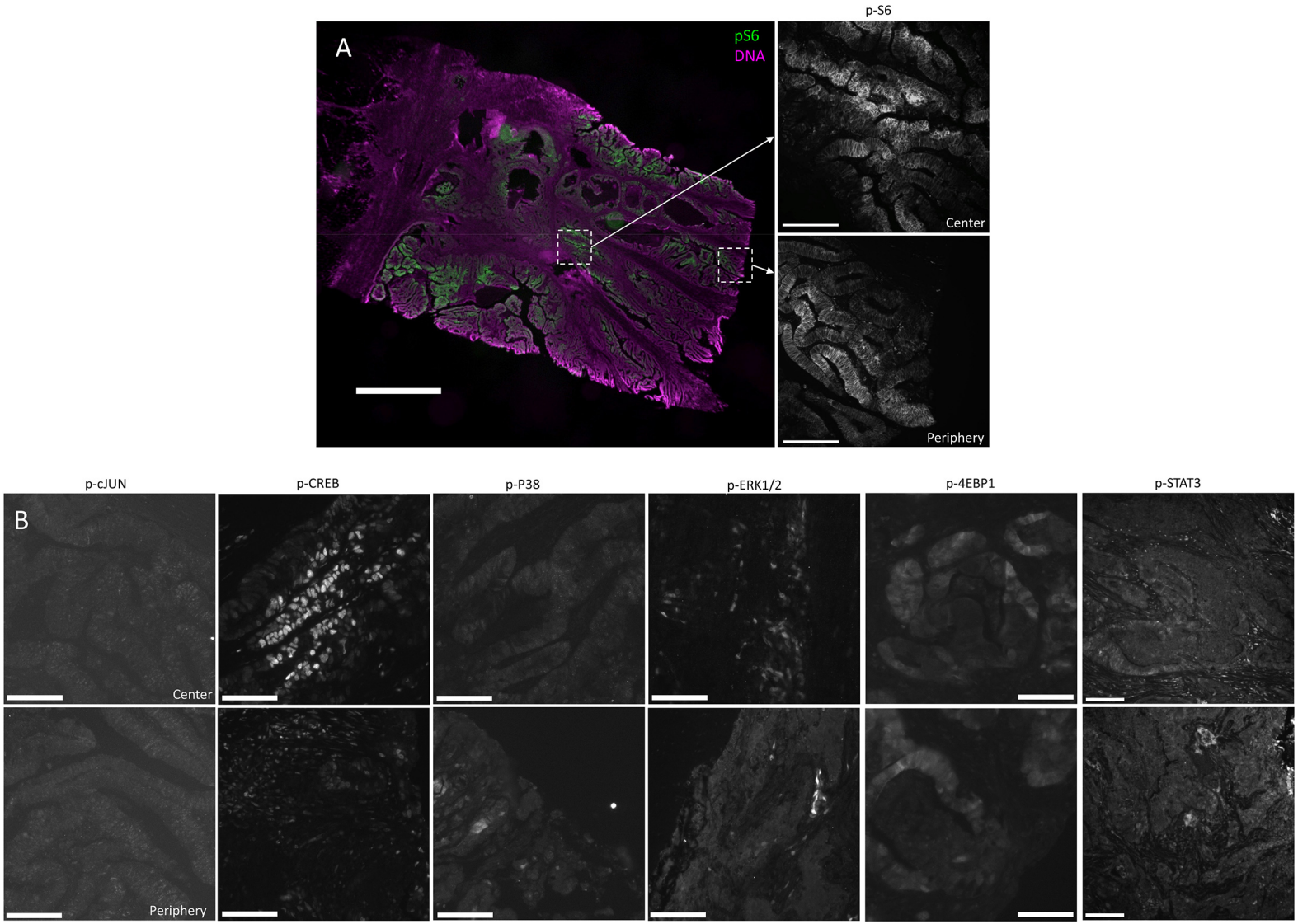

Fig. S13. Evidence of fixative penetration. (A) Demonstration of IF imaging of whole tumors at the periphery or center for p-S6. Scale bars, 2 mm for low magnification image, and 100 μm for insets. **(B)** Representative images of signaling markers detected at the periphery and the center of the same tumors. Scale bars, 100 μm. Data representative of n=13 tumor samples.

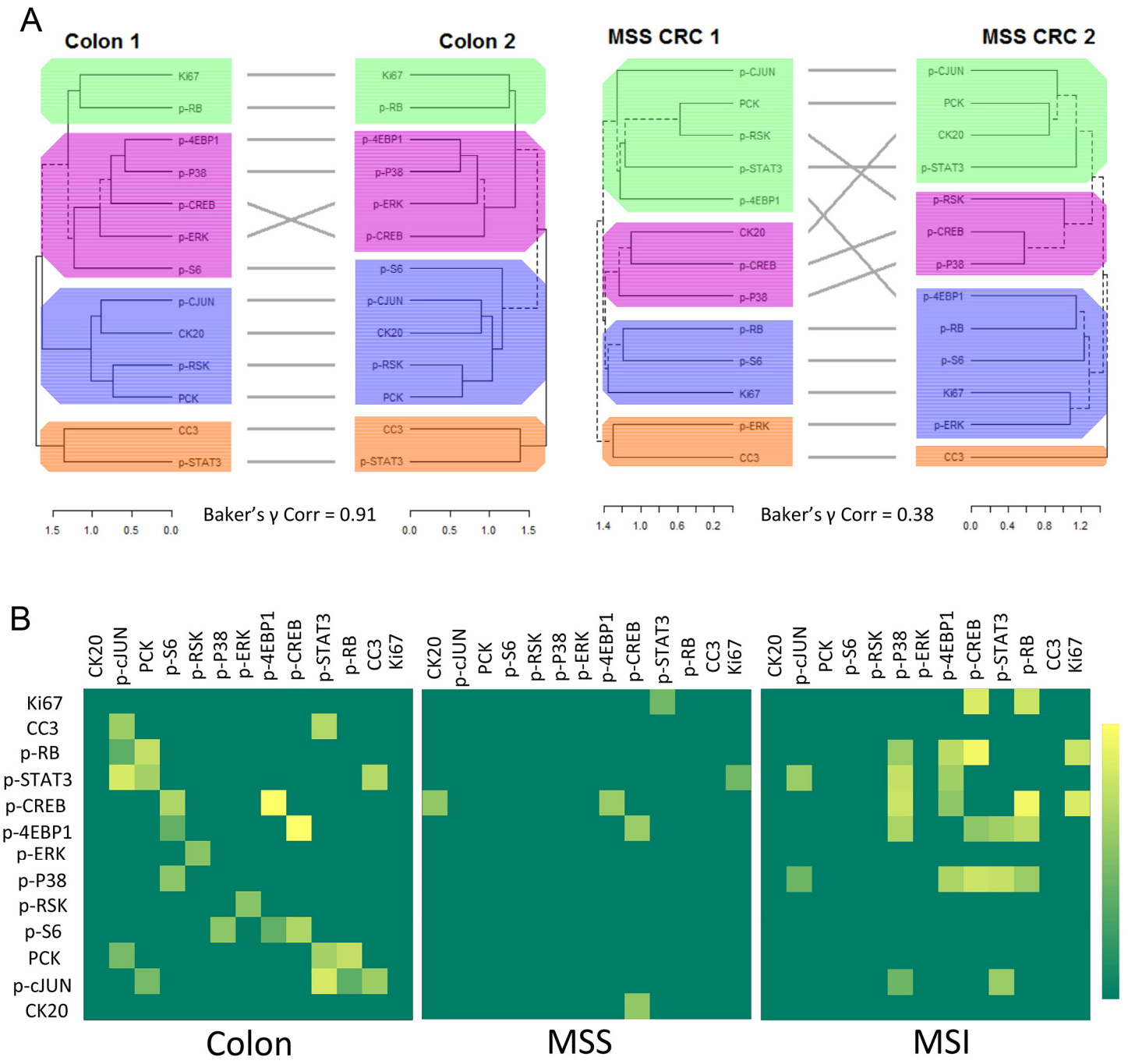
A
Colon 1
Colon 2
MSS CRC 1
MSS CRC 2
Ki67
p-RB
p-4EBP1
p-P38
p-CREB
p-ERK
p-S6
p-CJUN
CK20
p-RSK
PCK
CC3
p-STAT3
Baker's γ Corr = 0.91
Baker's γ Corr = 0.38
B
CK20
p-cJUN
PCK
p-S6
p-RSK
p-P38
p-ERK
p-4EBP1
p-CREB
p-STAT3
p-RB
CC3
Ki67
Colon
MSS
MSI

Fig. S14. Analysis of the organization of signaling pathways in human specimens. (A) Pairwise comparisons between hierarchical clustering trees with calculated Baker's gamma correlation coefficient for normal colon and MSS CRC. Colored blocks represent signaling modules as determined by clustering on signaling markers. **(B)** Heatmaps generated by pairwise correlations between signaling markers calculated over all samples, disregarding single-cell data but instead using the median values generated from single-cell distributions. Heat represents correlation >0.7. Data representative of n>6 human patient samples for each group (colon, MSS-CRC, MSI-CRC).

Epitope	Clone
CKAE1/3	CKAE1/AE3
p-4EBP1 (T37/46)	236B4
p-RB (S807/811)	D20B12
p-S6 (S240/244)	D68F8
p-ATF2 (T71)	11G2
p-P38 (T180/Y182)	D3F9
p-STAT3 (Y705)	D3A7
p-CJUN (S73)	D47G9
p-RSK (T359/S363)	D1E9
p-CREB (S133)	87G3
p-ERK1/2 (T202/Y204)	D13.14.4E
p-EGFR (Y1068)	D7A5
ChrgA	Polyclonal
CLCA1	EPR12254-88
C-Caspase 3 (N-175)	Polyclonal

Table S1. Mouse antibody reagent panel. Antibodies and their clone names used for evaluating specific markers in mouse mass cytometry studies.

ID	Age	Sex	Metastatic	Stage	Grade	KRAS	BRAF	MSI status	Tumor Site	PET (h)
33468	57	M	Yes	IIIC	G2	U	U	MSS	Sigmoid	1
33469	75	M	No	II	G2	U	U	MSS	Cecum and ileocecal valve	0.5
33470	56	F	Yes	IV	G3	G12V	WT	MSS	Cecum	1
33471	81	F	No	IIA	G2	U	V600E	MSI-H	Left colon	0.5
33472	47	M	Yes	III	G3	U	V600E	MSI-H	Cecum	0.5
33473	80	M	U	IIA	G2	WT	WT	MSS	Sigmoid colon	0.5
33474	78	F	U	IIA	G2	U	V600E	MSI-H	Hepatic flexture	0.5
33475	58	M	Yes	IIIB	G2	U	U	MSS	Right colon	0.5
33476	65	M	Yes	IV	U	U	WT	MSI-H	Cecum	0.75
33478	35	M	Yes	IIIC	G2	WT	U	MSS	Sigmoid colon	0.5
33479	40	M	U	IIA	G2	U	WT	MSI-H	Hepatic flexture	0.5
33482	71	M	Yes	IIIC	G2	G12C	WT	MSS	Lower pole	0.5
33483	82	M	Yes	IIIB	G3	U	V600E	MSI-H	Right colon	0.5

Table S2. Summary pathological characteristics of human colon cancer samples. A collection of CRC samples used for human studies with characteristics of patient age and sex, presence of metastasis, stage and grade of CRC, *KRAS* and *BRAF* mutation status, MSI status, site of tumor, and post-excision time in hours (PET).

Epitope	Clone
CK18	C-04
CD117 (KIT)	104D2
p-EGFR (Y1068)	D7A5
p-4EBP1 (T37/46)	236B4
p-RB (S807/811)	D20B12
p-S6 (S240/244)	D68F8
CD8	C8/144B
Vimentin	D21H3
p-P38 (T180/Y182)	D3F9
p-CJUN (S73)	D47G9
p-STAT3 (Y705)	D3A7
p-RSK (T359/S363)	D1E9
Pan-CK	C11
p-CREB (S133)	87G3
p-ERK1/2 (T202/Y204)	D13.14.4E
Ki-67	B56
CHGA	Polyclonal
CK20	D9Z1Z
CLCA1	EPR12254-88
C-Caspase 3 (N-175)	Polyclonal

Table S3. Human antibody reagent panel. Antibodies and their clone names used for evaluating specific markers in human mass cytometry studies.